materials

MDPI

Article

Observation of the Specific Heat Jump in the Se-Substituted $MoTe_2$ Single Crystals

Aoi Kobayashi, Yoshiki Takano and Satoshi Demura *

College of Science and Technology, Nihon University, Chiyoda-ku, Tokyo 101-8308, Japan; csao20009@g.nihon-u.ac.jp (A.K.); takano.yoshiki@nihon-u.ac.jp (Y.T.)
* Correspondence: demura.satoshi@nihon-u.ac.jp

Abstract: 1T′-$MoTe_2$ has gained considerable attention owing to its topological character. This material undergoes spatial inversion symmetry at 300 K. A structural transition to the T_d phase, which is represented by a kink in the resistivity, was observed below 250 K without inversion symmetry along the *c*-axis, while superconductivity was observed at 0.1 K. Substitution of Se into this material suppressed the appearance of the kink structure and increased the superconducting transition temperature to 2 K, which is consistent with previously reported results on polycrystalline samples. However, a specific heat jump was observed in the obtained single crystals, which did not exhibit kink structures in their resistivity. The results suggest that the T_d structure was not suppressed entirely after Se substitution and that superconductivity was achieved without inversion symmetry.

Keywords: superconductivity; transition metal chalcogenides; transport properties

check for updates

Citation: Kobayashi, A.; Takano, Y.; Demura, S. Observation of the Specific Heat Jump in the Se-Substituted $MoTe_2$ Single Crystals. *Materials* **2022**, *15*, 3782. https://doi.org/10.3390/ma15113782

Academic Editor: Naurang L. Saini

Received: 8 March 2022
Accepted: 7 May 2022
Published: 25 May 2022

Publisher's Note: MDPI stays neutral with regard to jurisdictional claims in published maps and institutional affiliations.

Copyright: © 2022 by the authors. Licensee MDPI, Basel, Switzerland. This article is an open access article distributed under the terms and conditions of the Creative Commons Attribution (CC BY) license (https://creativecommons.org/licenses/by/4.0/).

1. Introduction

Transition metal chalcogenides have been extensively studied owing to their unique properties. The properties of such compounds depend on crystal polymorphism. $MoTe_2$, which is a chalcogenide, may undergo different crystal polymorphisms: 2 H, 1T′, and T_d types [1–4]. The 2 H type represents a semiconducting electronic structure, whereas the 1T′ type implies a semimetallic state. The 1T′ type changes to the T_d type at temperatures below 250 K. The crystal structure of the T_d type does not have spatial inversion symmetry along the *c*-axis [1]. Owing to symmetry breaking, the T_d type has been predicted to be type-II Weyl semimetals [5]. Furthermore, the T_d type exhibits superconductivity at 0.1 K [6]. Therefore, 1T′- and T_d- type $MoTe_2$ are useful for topological physics research to determine the relationship between the topological character and superconductivity [7]. Superconductivity is enhanced via the application of pressure and element substitution [6,8–11]. However, avoiding a transition to the T_d type is also necessary. Because T_d-type suppression results in the recovery of inversion symmetry, the relationship between the enhancement and the topological state remain unclear. To resolve this issue, it is useful to confirm whether the structural phase-transition is suppressed in the bulk.

In this study, we performed specific heat measurements in Se-substituted $MoTe_{2-x}Se_x$ single crystals. The Se concentration was finely tuned in these crystals, which were prepared using the chemical vapor transport method. The kink in the resistivity curve related to the structural transition was observed at approximately 290 K for x = 0.0–0.12, and it was suppressed for x > 0.12. The onset of the superconducting transition temperature increased to approximately 3 K for x = 0.13–0.28. These results are similar to those previously reported for polycrystalline Se-substituted $MoTe_2$ [10]. Moreover, a specific heat jump for all samples was observed at approximately 290 K. This observation is similar to the observed kink for the x = 0.0–0.07 samples. These results indicate that the structural transition is not entirely suppressed. Therefore, the superconductivity is enhanced by maintaining the T_d-type structure possibility.

2. Experimental Details

Single crystals of $MoTe_{2-x}Se_x$ were prepared by chemical vapor transport. Mo (purity 99.9%), Te (purity 99.9%), and Se (99.9%) powders were used as raw materials. The aforementioned powders was used following the stoichiometric ratio of $MoTe_{2-x}Se_x$. The weight of these powders is 1 g. I_2 (5 g/ml) was used as the transport material. Owing to the volatility of I_2, it was weighed immediately before proceeding to the evacuation process. The raw materials and I_2 were sealed in an evacuated quartz tube (4.0×10^{-3} Pa). A three-zone horizontal electric furnace (ARF3-600, Asahi-rika Co., Chiba, Japan) was used to sinter the evacuated quartz tube. The thermal preparation process is illustrated in Figure 1a. The dimensions of the prepared samples were 2 × 3–5 mm^2, as depicted in Figure 1b. These crystals contained metallic silver, similar to the 1T′-$MoTe_2$ crystals previously reported. Additionally, these crystals easily glowed along the *b*-axis [4]. Therefore, the longitudinal direction corresponded to the *b*-axis, as shown in Figure 1b.

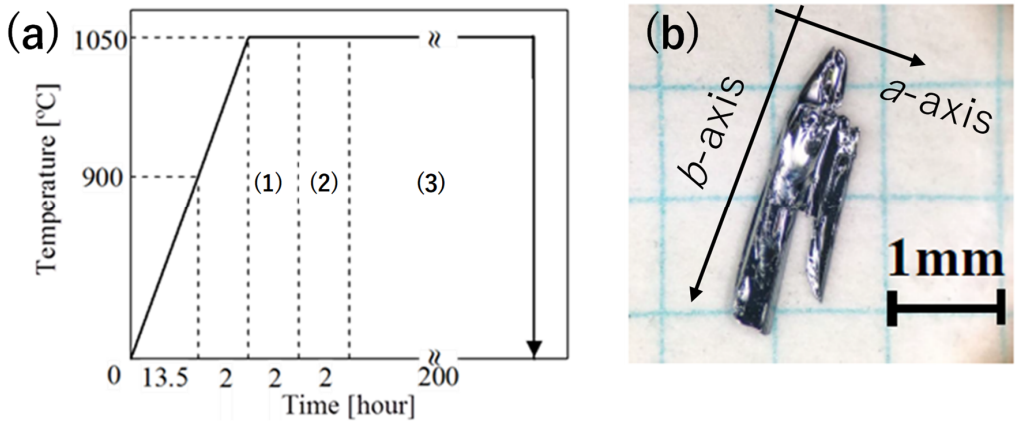

Figure 1. (**a**) Thermal conditions to obtain 1T′-$MoTe_2$. (1–3) indicate the stabilizing furnace, preparation slope, and temperature stability processes, respectively. At first, the furnace was heated up to 1050 °C for 15.5 h and maintained for 2 h for temperature stabilization (1). Next, the high and low-temperature ends were set to 1050 °C and 950 °C for 2 h, respectively (2). The temperature condition was maintained for 200 h (3). Thereafter, quartz tubes were immersed in water to avoid 2 H structure formation (hexagonal crystal), which is known to be stable at approximately 800 °C. (**b**) Image of the 1T′-$MoTe_2$ single crystal sample prepared by chemical vapor deposition.

X-ray diffraction (XRD, Ultima IV, Rigaku, Tokyo, Japan) measurements used by a Cu-Kα radiation (λ = 1.54056 Å) were performed for single and powdered samples, wherein the single crystals were ground. Simulation peaks were calculated using VESTA (version 3.4.4, Japan) [12]. Crystal structure data for 1T′-$MoTe_2$ were obtained from AtomWorks (http://crystdb.nims.go.jp/, accessed on 8 August 2019) [13]. Electron scanning microscopy (SEM, Hitachi High-Tech Fielding Corporation, Tokyo, Japan) and energy dispersive X-ray analysis (EDX, HORIBA, Tokyo, Japan) were conducted to investigate the compositions of the samples. The composition ratios of Mo, Te, and Se were determined, and the composition of Mo was normalized to 1. Electrical resistivity and specific heat were measured using a Physical Property Measurement System (PPMS, Quantum Design, Takamatsu, Japan). Because the resistivity values for the $MoTe_2$ samples are relatively low, a four-terminal method was adopted. The temperature range was set to 2–300 K. A heat relaxation method was used for specific heat measurements in the range of 3–300 K.

3. Result and Discussion

XRD measurements were performed on $MoTe_{2-x}Se_x$ single crystals and powders. The results for both set of samples are presented in Figure 2. The observed peaks were indexed via comparison with the 1T′-type structure simulation. Consequently, the results confirmed that 1T′-$MoTe_{2-x}Se_x$ single crystals were successfully obtained.

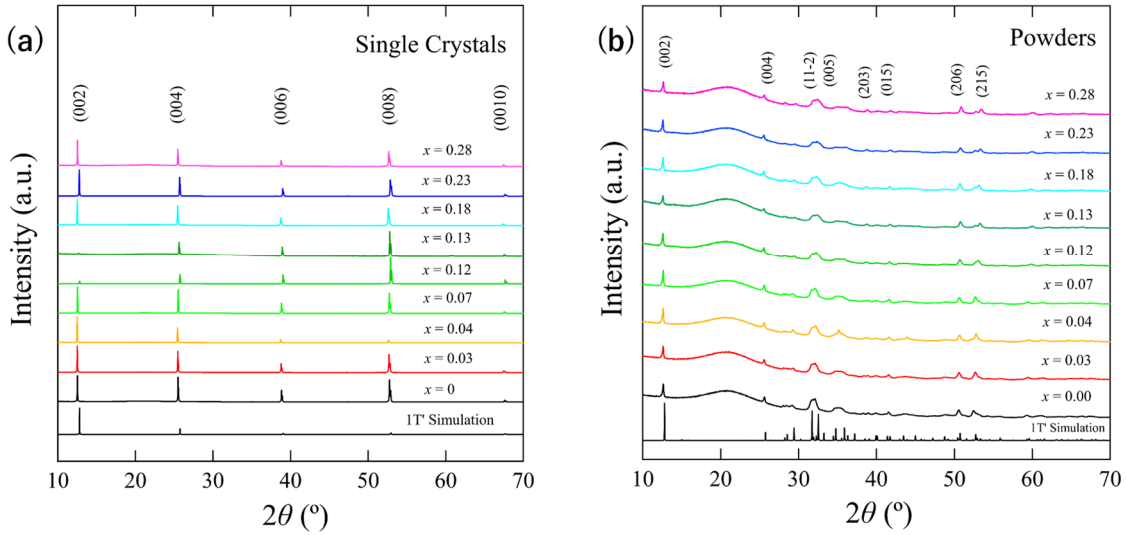

Figure 2. Results of XRD measurements of $MoTe_{2-x}Se_x$ samples with (**a**) single crystals and (**b**) powders. Simulation peaks were calculated using VESTA (version 3.4.4, Japan) [12] and crystal data were obtained from AtomWorks (http://crystdb.nims.go.jp/, accessed on 8 August 2019) [13]. The Se concentration (x) was obtained by EDX.

The dependence of the lattice constant on the Se concentration (x) along the c-axis is depicted in Figure 3. Lattice constants were determined for the (00l) (red open circles) and (008) (blue open circles) peaks. The (008) peaks contribute less to the error resulting from the difference in the sample shape, such as the height or roughness of the surface. When Se ions were substituted, the lattice constant along the c-axis expects to decrease because the ionic radius of Se is smaller than that of Te. However, the lattice constant was almost constant for all the samples; hence, the lattice constant was not Se-concentration dependent. These results are similar to those reported for S-substituted single crystals and Se-substituted polycrystals [8,10].

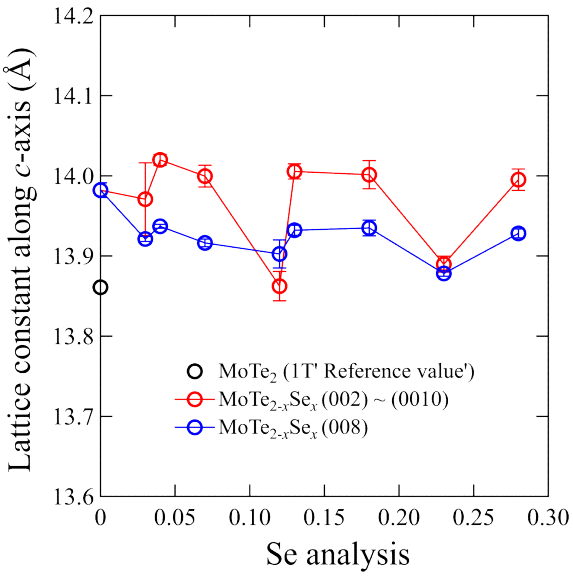

Figure 3. Lattice constants along the c-axis calculated through XRD patterns of the (00l) plane for single crystals. Error bars were calculated using five samples from the same batch. The reference value curve corresponds to previously reported results [14].

The dependence of the electrical resistivity on temperature for the single crystal samples is illustrated in Figure 4. For Se concentration (x) between 0–0.12 (Figure 4a), a kink and

hysteresis related to the structural phase transition to the T_d type can be observed during the thermal cycle at approximately 250 K at x = 0–0.04. This kink was suppressed gradually at x = 0.07 and 0.12. In addition, the temperature at which the kink was observed (T_s) differed according to the substitution of Se ions. Samples demonstrating a curve kink (x = 0–0.04) did not exhibit a superconducting transition, as shown in Figure 4b. The rest of the samples exhibited the onset of T_c at approximately 3 K. Moreover, the resistivity drop was small (~10% from the normal state), indicating the emergence of superconductivity below 2 K. As the Se concentration increased (x > 0.12), the kink in the curve was entirely suppressed (Figure 4c). Furthermore, samples with x = 0.13–0.28 exhibited superconductivity at approximately 3 K, as depicted in Figure 4d. These results indicate that Se substitution suppressed the kink gradually and induced an increase in Tc. Furthermore, Se substitution in polycrystalline $MoTe_2$ has been reported to suppress the structural phase transition at approximately 250 K; moreover, it has been reported to result in an increase in the onset of T_c to 3 K [10]. These results are similar to the results presented herein.

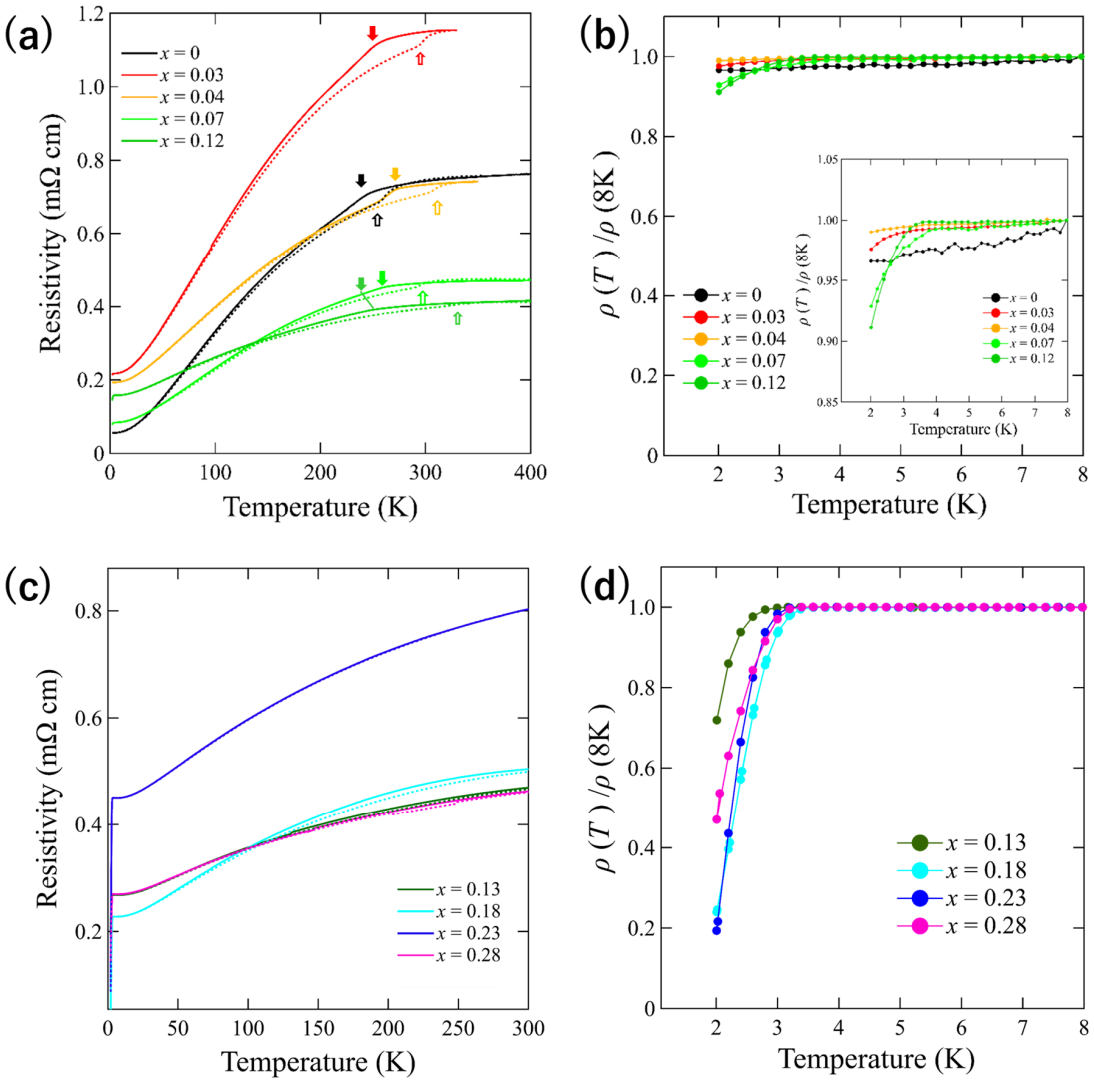

Figure 4. Temperature dependence of electrical resistivity for $MoTe_{2-x}Se_x$ single crystals. The results for x = 0–0.12 and x = 0.13–0.28 have been reported. (**a**,**c**) depict results in the entire temperature range. The solid and dotted lines correspond to the cooling and heating processes, respectively. Arrows indicate the temperature at which the kink appears (T_s). Filled and open arrows in (**a**) indicate T_s for the heating and cooling processes, respectively. (**b**,**d**) illustrate the region below 8 K, normalized by the resistivity at 8 K. The inset of (**b**) represents the magnified image (**b**) near the superconducting transition.

The superconducting state of the materials was investigated using resistivity measurements under magnetic fields. The sample prepared with $x = 0.28$ was selected for this purpose. Measurements were performed by applying magnetic fields and currents along each axis because the sample exhibited different in-plane axes. Therefore, two measurements were performed when the magnetic field and current were applied along the *a*-axis and *b*-axis. Because the transition was gradually suppressed when applying a magnetic field in both measurements, it could be concluded that this transition was related to superconductivity. The temperature dependence of $\mu_0 H_{c2}$ for all measurements is summarized in Figure 5a,b. T_c at each magnetic field was defined as the temperature at which the resistivity reached 90% of the normal-state resistivity. This T_c was denoted as $T_c^{90\%}$. The estimated $\mu_0 H_{c2}$ (0) values for all experimental conditions are summarized in Table 1. The value of $\mu_0 H_{c2}{}^{WHH}$, calculated from the Werthamer–Helfand–Hohenberg (WHH) model, was 2.4–3.8 T [15,16]. The Pauli limit, denoted as $\mu_0 H_c{}^{Pauli}$, was 4.8–5.4 T, which was calculated using $T_c{}^{90\%}$. Thus, $\mu_0 H_{c2}{}^{WHH}$ was lower than $\mu_0 H_c{}^{Pauli}$ for each condition. This tendency is consistent with that observed in previously reported high-pressure and element-substitution studies [6,10,11].

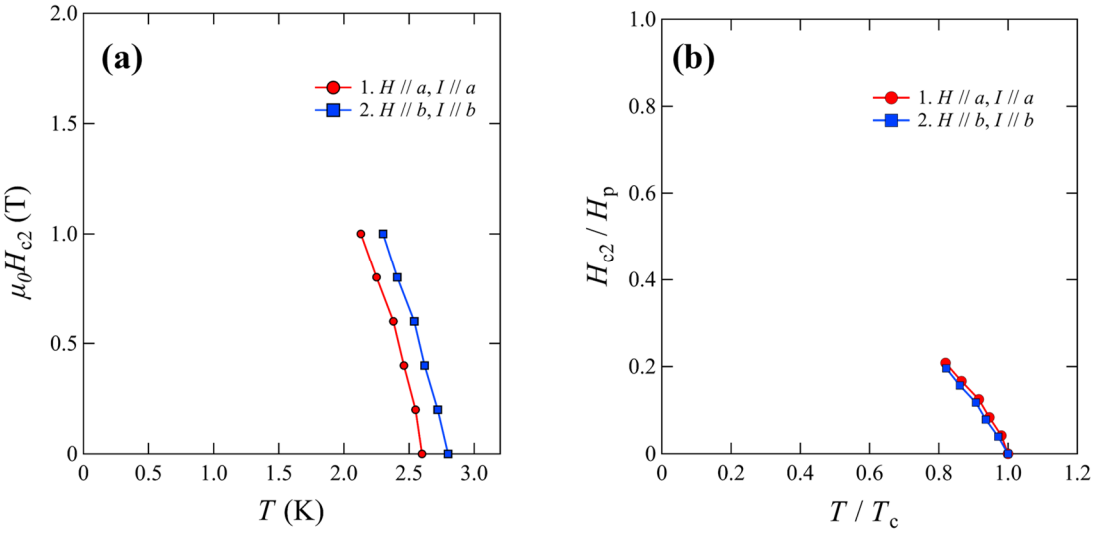

Figure 5. (**a**) Temperature dependence of the upper critical magnetic field. (**b**) illustrates (**a**) using normalized axes. Vertical and horizontal axes were normalized using Pauli's limit H_p and T_c, respectively.

Table 1. T_c and H_{c2} values estimated by the WHH model and the Pauli limit.

$T_c{}^{90\%}$ (K)	$-dH_{c2}/dT$	$\mu_0 H_{c2}{}^{WHH}$ (T)	$\mu_0 H_{c2}{}^{Pauli}$ (T)
2.9	1.2	2.4	5.3
2.6	2.1	3.7	4.8
3.0	1.2	2.4	5.4
2.8	2.0	3.8	5.1

Specific heat measurements were performed on the Se-substituted samples to investigate structural changes and to obtain electronic structure information. The results for the low-temperature region (below 50 K) are presented in Figure 6. These data were fitted using Equation (1), which describes the temperature dependence of the metal:

$$C(T)/T = \beta + \gamma T^2 \quad (1)$$

where β and γ denote fitting parameters. The parameters used are listed in Table 2. Neither parameter was dependent on the Se concentration except for $x = 0.28$. The samples with $x = 0.28$ exhibited slightly higher parameter values among all the other samples. However,

this difference was insignificant and did not affect properties. Indeed, the metallic behavior and T_c values did not exhibit significant changes. Thus, it can be concluded that a significant change in the electronic structure does not occur due to Se substitution. This result indicates that the increase in T_c was not related to an increase in the density of states near the Fermi energy. This observation is qualitatively consistent with previously reported data for S-substituted single crystals and Se-substituted polycrystals [8,10].

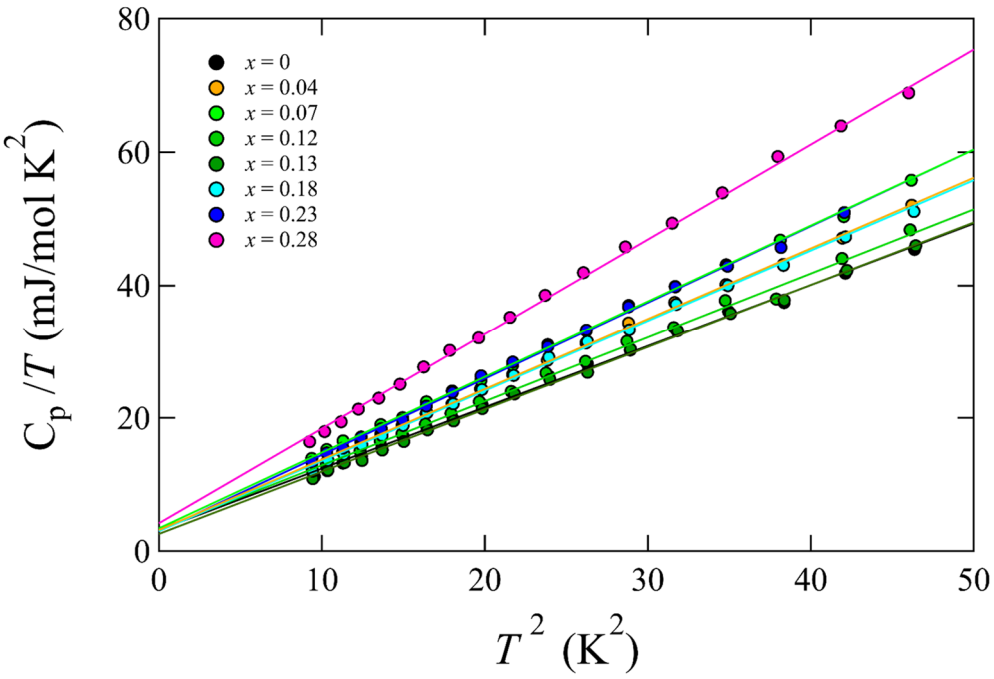

Figure 6. C_p/T as a function of T^2 for the single crystal samples. Each solid line indicates a fitting.

Table 2. Fitting parameters used in Figure 6.

Se Concentration (%)	β (mJ/mol K^4)		γ (mJ/mol K^2)	
0	3.2	(3)	0.92	(1)
0.04	3.2	(2)	1.06	(1)
0.07	3.4	(2)	1.14	(1)
0.12	3.3	(4)	0.97	(1)
0.13	2.6	(2)	0.94	(1)
0.18	3.0	(3)	1.06	(1)
0.23	3.0	(3)	1.15	(1)
0.28	4.2	(4)	1.42	(1)

The temperature dependence of specific heat (C_p) is illustrated in Figure 7a. It can be observed that the behavior is metallic at T < 200 K. A C_p jump can be observed at approximately 290 K until x = 0.23, after which it is gradually suppressed at x = 0.28 (Figure 7b). This temperature is consistent with the temperature corresponding to the appearance of a kink structure in the resistivity measurements for the x = 0–0.12 samples. Although the kink was suppressed above x = 0.13 in the resistivity curve, a jump in the heat capacity was observed above x = 0.13. These results can be attributed to either of two possibilities: phase separation in the sample or remnant of the T_d type. Although phase separation was not entirely excluded, composition analysis via EDX did not support this possibility. The composition of each sample (size 2–3 mm^2) was determined based on an average of five different measurements. The measured values at each location were almost constant, which demonstrated that the substituted Se ions were uniformly distributed. It should be noted that the T_d type was not completely suppressed by Se substitution.

Therefore, it is possible that the superconductivity observed at x = 0.13–0.28 appeared in the T_d type. The x = 0.28 sample exhibited a small jump at 290 K, whereas a kink and a slight jump were observed at approximately 230 K and 100 K, respectively (open triangles in Figure 7a). The sample with x = 0.07 also exhibited a slight kink, which indicates the appearance of new phases at this Se concentration. However, the underlying cause responsible for these phenomena requires further investigation.

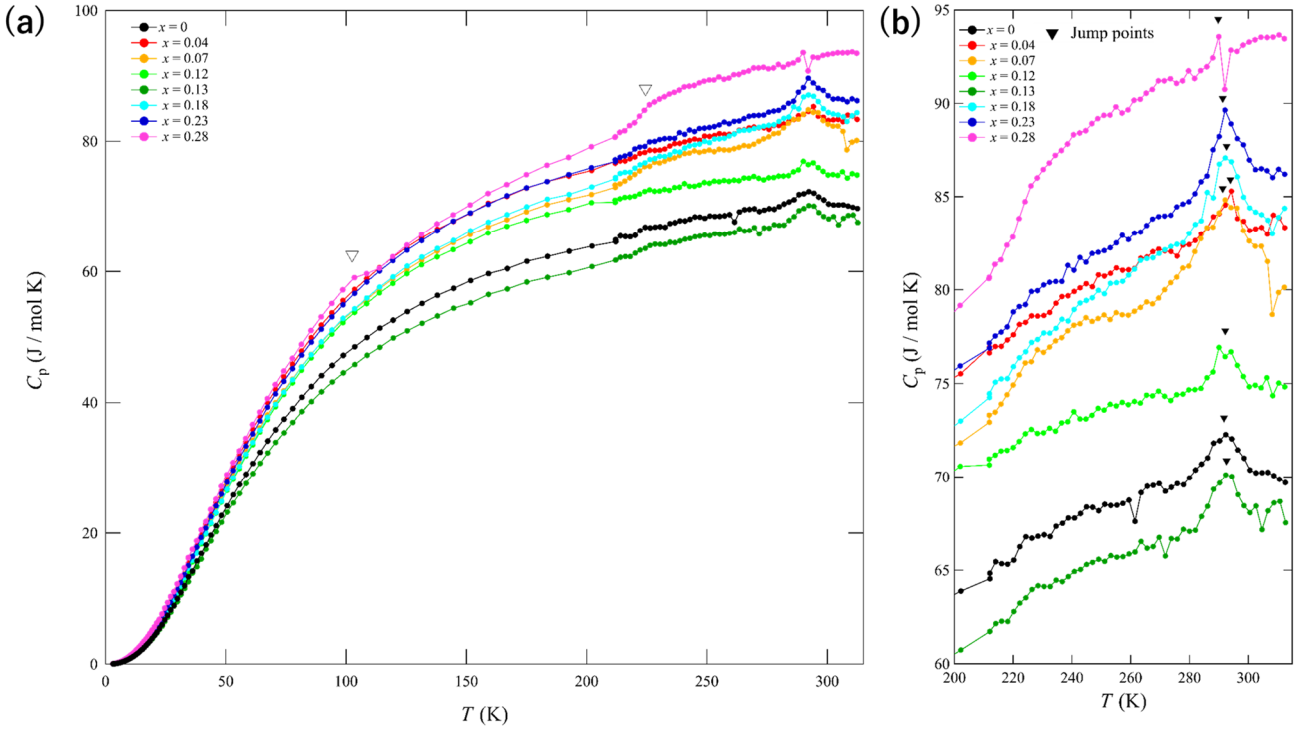

Figure 7. Temperature dependence of the specific heat (C_p) for single crystals. (**a**) in the operating temperature range and (**b**) in the temperature range of 200–310 K. Open triangles indicate unknown small jumps. Solid triangles in (**b**) indicate C_p jumps related to structural transitions.

The obtained results are summarized as a phase diagram in Figure 8 and in Table 3. Se substitution induced suppression of the kink observed in the resistivity for Se concentrations x > 0.12. After suppression, superconductivity at a higher T_c (approximately 3 K) occurred immediately. This result indicates that kink suppression is related to superconductivity enhancement. However, a heat capacity jump emerged, which was observed near the kink temperature at x = 0–0.12. This result demonstrated that phase transition to T_d type was not entirely suppressed, and a higher T_c phase was observed in the T_d type. Scanning tunneling microscopy measurements have recently been performed on Se-substituted $MoTe_2$ single crystals [17]. Consequently, superconductivity was observed at T_c^{onset} ~ 3 K; however, a kink structure was not observed. In contrast, a topographic image of the T_d type was observed at a cleaved surface. Raman measurements indicated the existence of the T_d type at low temperatures. From these results, it can be concluded that the observed jump in the specific heat value is presumably related to the T_d type transition in the bulk. Further investigations are, however, required for Se-substituted $MoTe_2$ with regard to the observation of the crystal structure at low temperatures via XRD measurements or through electronic structures.

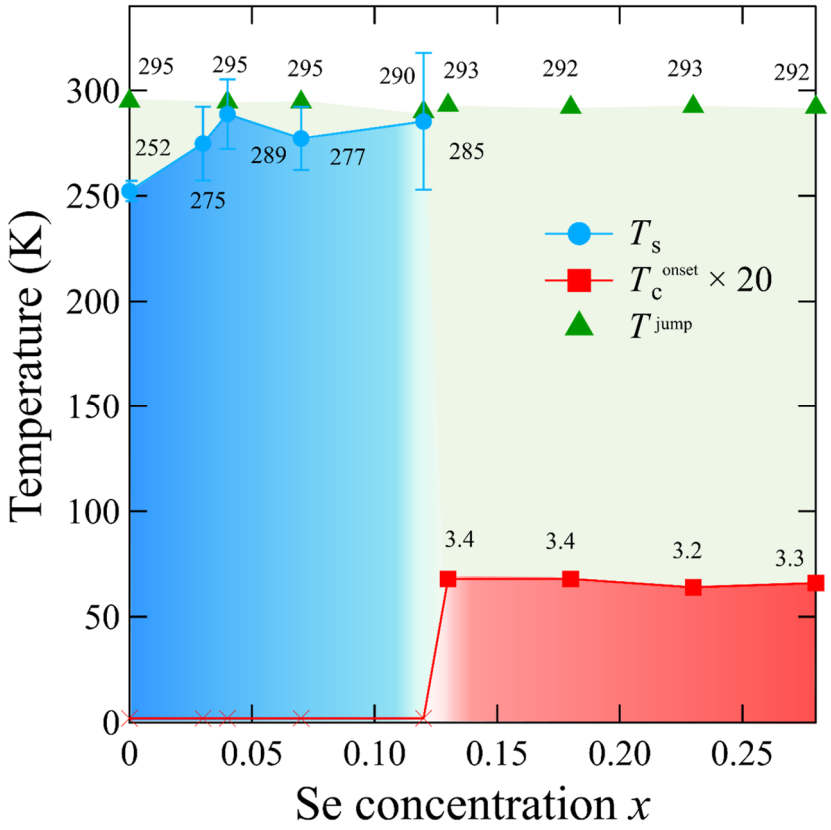

Figure 8. Phase diagram of the kink and superconductivity of the $MoTe_{2-x}Se_x$ single crystal. T_s denotes the temperature that corresponds to the kink in the resistivity curve. The bars represent the temperature corresponding to the kink, which is estimated in the heating and cooling processes. T^{jump} denotes the temperature attributed to the jump in specific heat. Red cross marks (×) indicate no superconductivity until 2 K.

Table 3. T_c^{onset}, T_c^{jump}, and T_s values used in Figure 8. Hyphen (-) indicates that no transition was observed. N.D. implies that no measurement was performed.

Se Concentration (%)	T_c^{onset} (K)	T^{jump} (K)	T_s (K)		
			Cooling	Heating	Ave.
0	-	295	247	257	252
0.03	-	N. D.	257	292	275
0.04	-	295	272	305	289
0.07	-	295	262	292	277
0.12		290	253	318	285
0.13	3.4	293	-	-	-
0.18	3.4	292	-	-	-
0.23	3.2	293	-	-	-
0.28	3.3	292	-	-	-

4. Conclusions

In this study, Se-substituted $MoTe_2$ single crystals were successfully prepared and evaluated. Resistivity measurements confirmed that Se substitution suppressed the appearance of the kink and induced a relatively higher T_c (approximately 3 K). The results were analogous to those previously reported for polycrystalline structures. However, a jump in the specific heat capacity was observed at approximately 250–290 K, which was independent of the Se concentration in the crystal. In resistivity measurements, the temperature was similar to that resulting in a kink for the $MoTe_{2-x}Se_x$ sample (x = 0–0.12). This result

demonstrated that the T_d type without spatial inversion symmetry along the *c*-axis was not completely suppressed, and a high T_c was obtained in the T_d type. We believe that this study may be significant for investigations on the topological physics of Weyl semimetals.

Author Contributions: Conceptualization, A.K., Y.T. and S.D; methodology, S.D.; validation, A.K., Y.T. and S.D.; resources, Y.T. and S.D; writing—review and editing, Y.T. and S.D.; visualization, A.K. and S.D.; funding acquisition, Y.T. and S.D.; Data curation, A.K.; Formal analysis, A.K.; Investigation, A.K. and S.D.; Project administration, S.D.; Supervision, Y.T.; Writing–original draft, S.D. All authors have read and agreed to the published version of the manuscript.

Funding: This work was partly supported by a Grant-in-Aid for Young Scientists (JP18K13505) in a Grant-in-Aid for Scientific Research (KAKENHI) from the Japan Society for the Promotion of Science (JSPS). This work was partly supported by a grant for research from Nihon University (College of Science and Technology) and a grant for special research from the President of Nihon University.

Conflicts of Interest: The authors declare no conflict of interest.

References

1. Clarke, R.; Marseglia, E.; Hughes, H.P. A low-temperature structural phase transition in β-MoTe2. *Philos. Mag. B* **1978**, *38*, 121–126. [CrossRef]
2. Puotinen, D.; Newnham, R.E. The crystal structure of MoTe2. *Acta Cryst.* **1961**, *14*, 691–692. [CrossRef]
3. Zandt, T.; Dwelk, H.; Janowitz, C.; Manzke, R. Quadratic temperature dependence up to 50 K of the resistivity of metallic MoTe2. *J. Alloys Compd.* **2007**, *442*, 216–218. [CrossRef]
4. Yan, X.J.; Lv, Y.Y.; Li, L.; Li, X.; Yao, S.H.; Chen, Y.B.; Liu, X.P.; Lu, H.; Lu, M.H.; Chen, Y.F. Investigation on the phase-transition-induced hysteresis in the thermal transport along the c-axis of $MoTe_2$. *NPJ Quantum Mater.* **2017**, *2*, 31. [CrossRef]
5. Sun, Y.; Wu, S.C.; Ali, M.N.; Felser, C.; Yan, B. Prediction of Weyl semimetal in orthorhombic MoTe 2. *Phys. Rev. B* **2015**, *92*, 161107. [CrossRef]
6. Qi, Y.; Naumov, P.G.; Ali, M.N.; Rajamathi, C.R.; Schnelle, W.; Barkalov, O.; Hanfland, M.; Wu, S.C.; Shekhar, C.; Sun, Y.; et al. Superconductivity in Weyl semimetal candidate MoTe2. *Nat. Commun.* **2016**, *7*, 11038. [CrossRef] [PubMed]
7. Luo, X.; Chen, F.C.; Zhang, J.L.; Pei, Q.L.; Lin, G.T.; Lu, W.J.; Han, Y.Y.; Xi, C.Y.; Song, W.H.; Sun, Y.P. Td-MoTe2: A possible topological superconductor. *Appl. Phys. Lett.* **2016**, *109*, 102601. [CrossRef]
8. Chen, F.C.; Luo, X.; Xiao, R.C.; Lu, W.J.; Zhang, B.; Yang, H.X.; Li, J.Q.; Pei, Q.L.; Shao, D.F.; Zhang, R.R.; et al. Superconductivity enhancement in the S-doped Weyl semimetal candidate MoTe2. *Appl. Phys. Lett.* **2016**, *108*, 162601. [CrossRef]
9. Guguchia, Z.; von Rohr, F.; Shermadini, Z.; Lee, A.T.; Banerjee, S.; Wieteska, A.R.; Marianetti, C.A.; Frandsen, B.A.; Luetkens, H.; Gong, Z.; et al. Signatures of the topological s +- superconducting order parameter in the type-II Weyl semimetal T d-MoTe 2. *Nat. Commun.* **2017**, *8*, 1082. [CrossRef] [PubMed]
10. Takahashi, H.; Akiba, T.; Imura, K.; Shiino, T.; Deguchi, K.; Sato, N.K.; Sakai, H.; Bahramy, M.S.; Ishiwata, S. Anticorrelation between polar lattice instability and superconductivity in the Weyl semimetal candidate MoTe 2. *Phys. Rev. B* **2017**, *95*, 100501. [CrossRef]
11. Mandal, M.; Marik, S.; Sajilesh, K.P.; Arushi; Singh, D.; Chakraborty, J.; Ganguli, N.; Singh, R.P. Enhancement of the superconducting transition temperature by Re doping in Weyl semimetal MoTe 2. *Phys. Rev. Mater.* **2018**, *2*, 094201. [CrossRef]
12. Momma, K.; Izumi, F. VESTA 3 for three-dimensional visualization of crystal, volumetric and morphology data. *J. Appl. Crystallogr.* **2011**, *44*, 1272–1276. [CrossRef]
13. Xu, Y.; Yamazaki, M.; Villars, P. Inorganic materials database for exploring the nature of material. *Jpn. J. Appl. Phys.* **2011**, *50*, 11RH02. [CrossRef]
14. Brown, B.E. The crystal structures of WTe2 and high-temperature MoTe2. *Acta Cryst.* **1966**, *20*, 268. [CrossRef]
15. Maki, K. Effect of Pauli paramagnetism on magnetic properties of high-field superconductors. *Phys. Rev.* **1966**, *148*, 362. [CrossRef]
16. Helfand, E.; Werthamer, N.R. Temperature and purity dependence of the superconducting critical field, H c 2. II. *Phys. Rev.* **1966**, *147*, 288. [CrossRef]
17. Wang, Z.; Olivares, J.; Namiki, H.; Pareek, V.; Dani, K.; Sasagawa, T.; Madhavan, V.; Okada, Y. Visualizing superconductivity in a doped Weyl semimetal with broken inversion symmetry. *Phys. Rev. B* **2021**, *104*, 115102. [CrossRef]